

Type of the Paper (Article)

The potential use of geophysical methods to identify cavities, sinkholes and pathways for water infiltration: a case study from Mambaí, Brazil

Yawar Hussain^{1*}; Rogerio Uagoda²; Welitom Borges³; José Nunes²; Omar Hamza⁴; Cristobal Condori³; Khurram Aslam⁵; Jie Dou⁶; Martín Cárdenas-Soto⁷

¹ Environmental Engineering and Earth Science Department, Clemson University, Clemson, USA

² Department of Geography, University of Brasilia, Brasilia, Brazil

³ Institute of Geoscience, University of Brasilia, Brasilia, Brazil

⁴ Department of Built Environment, University of Derby, Derby, UK

⁵ Department of Earth Sciences, University of Oregon, Oregon, USA

⁶ Department of Civil and Environmental, Nagaoka University of Technology, Niigata, Japan

⁷ Department of Geophysical Engineering, National Autonomous University of Mexico, México

* Correspondence: yawar.pgn@gmail.com

Abstract: The use of geophysical characterization of karst systems can provide an economical and non-invasive alternative for extracting information about cavities, sinkholes, pathways for water infiltration as well as the degree of karstification of underlying carbonate rocks. In the present study, three geophysical techniques, namely, Ground Penetrating Radar (GPR), Electrical Resistivity Tomography (ERT) and Very Low Frequency Electromagnetic (VLFEM) were applied at three different locations in relation to fluvial karst, which is listed as an environmentally sensitive area in Rio Vermelho, Mambaí, Goiás, Brazil. In the data acquisition phase, the GPR, direct-current (DC) resistivity and VLFEM profiles were obtained at the three locations in the area. Data were analyzed using commonly adopted processing workflows. Different radar typologies have been assigned to soil and rock types. The GPR results showed a well-defined lithology of the site based on the amplitude of the signal. On the other hand, the inverted resistivity cross-sections showed a three-layered stratigraphy, pathways of water infiltration and the weathered structures in carbonate (Bambui group). The interpretation of VLFEM as contours of current density resulted from Fraser and Karous-Hjelt filters, indicate the presence of conductive structures (high apparent current density) that may be linked with the weathered carbonate and other conductive and resistive anomalies may be associated with the water-filled and dry cavities (cave). The results encourage the integrated application of geophysical techniques as the reconnaissance for further detailed characterization of the karst areas.

Keywords: Tarimba cave; conductive zones; karst; radar typologies

1. Introduction

Karst processes often resulted in underground natural cavities due to the erosive effect of groundwater (dissolution) on carbonate rocks (Abidi et al. 2018). These features may develop caves with time which may or may not reach the surface creating sinkholes (Mohamed et al. 2019). Such karst processes can significantly impact people's lives because they may cause severe damage to properties and infrastructures including road subsidence, building-foundation collapse, dam leakage, and groundwater contamination (Gambetta et al. 2011; Youssef et al. 2016). In practice, these underground cavities and other karst features must be detected before the construction of any civil structures or groundwater management schemes. Another critical aspect of these caves lies in the fact that it can provide a safe and consistent habitat for particular species. Therefore, early and accurate detection of the subsurface karst conditions can play an essential role in environmental and geohazard risk assessments.

Karst areas are the subject of a broad range of studies such as archaeological, environmental hydrogeological, geological, geotechnical and geomorphological. These studies provide incomplete information about the degree of karstification without adequate data of the internal structures of the area e.g. epikarst, infiltration zones, karst conduits, cavities, presence and type of overlying sediments and thickness. The analysis of internal structures and geometry of karst is a challenging task because of the uncertainties created by the karst heterogeneities. Though, the knowledge of internal karst structures is highly essential for the vulnerability assessment of the karst aquifers (infiltration-property distribution) because it influences the infiltration conditions and other environmental aspects. The presence and thickness of overlying sediments can slower and diffuse infiltration, while the presence of

holes or dolines and the absence of soil cover can expedite this process (Daly et al. 2002; Andreo et al. 2009; Kavouri et al. 2011). Therefore, accurate detection of such voids is valuable.

For the subsurface identification and mapping of a sinkhole, the non-invasive and high-resolution geophysical techniques have appeared as an appropriate choice (Smith, 1986; Zhou et al. 2002; Al-Tarazi et al., 2008; Ezersky, 2008; Krawczyk et al. 2012; Martinez-Moreno et al. 2013; Argentieri et al. 2015; Pazzi et al. 2018). In the case of natural cavities, which are usually filled with either water, air or collapsed material create contrast in physical properties in comparison to the surrounding rocks. This physical contrast can be detected with the application of geophysical techniques (Bishop et al. 1997). The onset of cavities leads to the disturbance in the surrounding rocks, which are extended away from the cavity (Pazzi et al. 2018).

There is a wide range of geophysical methods, for example, Ground Penetrating Radar (GPR), Electrical Resistivity Tomography (ERT) and Very Low Frequency Electromagnetic (VLFEM) are considered to be appropriate techniques for the delineation of conductive and resistive structures in the subsurface (Dourado et al. 2001; Sharma and Baranwal, 2005; Chalikakis et al. 2011; Abbas et al. 2012; Ozegin et al., 2012; Martinez-Lopez et al. 2013; PUTIŠKA et al. 2014; Ammar and Kruse, 2016; Čeru et al. 2017; Fabregat et al. 2017; Putiška et al. 2017; Jamal and Singh, 2018; Pazzi et al. 2018). Over the past couple of decades, the applications of GPR in the karst studies have increased many improvements have been successfully implemented (Ehsani et al. 2008). It has applied for the identification as well as in delineation of cave geometries, is very important in understanding karstification and speleogenetic processes that may contain useful information required for the reconstruction of the former underground water flows (Čeru et al. 2018). All of these methods are capable of providing high-resolution images of the subsurface settings and can also be used to distinguish between different types of sedimentary fillings in the cavities (Pazzi et al. 2018).

Karst terrains are widespread in Brazil especially, in the central and eastern regions of the country, where carbonate karst occurs and are characterized by horizontally bedded and dolomite limestone

having little or no relief developed under the influence of seasonal climatic variations (Auler and Farrant, 1996). The caves are broadly divided into two main groups as carbonated karst and non-carbonated karst of which carbonated karst is relatively more studied, however, the study of karst in Brazil is still in the infancy stage and require further detailed analysis (Auler and Farrant 1996). The prominent karst studies in Brazil are dos Santos et al. 2012; de Queiroz et al. 2018 and Garcia et al. 2019.

The present study applies geophysical techniques for the site characterization of the Tarimba cave, which has not been previously conducted at this site, thereby provide potential material for future detailed field campaigns. The geophysical investigations were conducted at three different sites on the karst system aiming to show the potential of the methods to identify cavities, sinkholes or paths for water infiltration. For the data acquisition, this presents an ideal site, having limestone exposures, limited or no soil cover and vegetation, and underlying shallow caves in a semi-arid region, where the karst system is dry during most of the year. Such non-invasive site characterization is crucial in environmentally sensitive areas for the identification of cavities, sinkholes (open or filled), pathways for water infiltration and delineation of the weathered carbonate structures. The study provides a sound basis and recommendations for future investigation to improve the characterization of the Brazilian karst and about the geogenic protection to its underlying environment.

2. Study area and investigation methods

2.1 Study area

The study area is located at the junction of the municipality of Mambaí, and has geographic coordinates: UTM 23L 373343 longitude 8406394 latitude (Figure 1). The Tarimba cave (which is the target of this study) has many entries and is approximately 11 km in length and partially mapped into several conduits and halls. Tarimba is considered one of the most important caves in the region and also one of the largest in the country in terms of horizontal projection. The climate of the region is

tropical with dry and rainy seasons. In the area, there are numerous rivers such as Currente, Vermelho and Buritis. The main streams flowing the area are Bezerra, Piracanjuba, Rizada, Chumbada and Ventura. Some watercourses penetrate into the soil becoming subterranean and later surfacing, promoting the formation of caves (Lobo et al. 2015; de Souza Martinelli et al. 2015). The northeastern region of the State of Goiás has several geomorphological domains. Their features are evidenced by the morphostructure climate reworked, contrasting dissected and recessed forms interposed conserved forms, which represent remnants of the oldest topography. It is drained by the Paraná and Maranhão Rivers, which forms the Tocantins River (Lobo et al. 2015).

The northeast region of Goiás presents lands with stratigraphic records of the Archaean, Proterozoic, Mesozoic and Cenozoic, most of which Proterozoic, which includes the following units: Ticunzal formation, sequence volcanic-sedimentary rocks of Palmeirópolis and São Domingos, Arai group, Serra Branca, Tonalito São Domingos, Paranoá group and Bambuí group. The most extensive carbonate unit is the Bambuí Group, which hosts the largest number of caves in Brazil (Auler, 2002). The Urucua formation representing continental fluvial deposition, restricted to the eastern portion of the area, attributed to the Cretaceous, land of Mesozoic age. The Cenozoic is represented by the current fluvial deposits, alluvial and colluvial sandy deposits and by the detritus-lateritic cover.

The previous geological studies have pointed out the presence of rocks from the Urucua group, without having details about the individual geological formations there. The field activities made it possible to individualize formations, as fine matrix Sandstone (quartzstone), white in color having large cross-stratification, an indicator of the deposition by the wind. This is overlain by the *Serra das Araras* formation containing reddish sandstones with the hills supported by thick layers of laterite, with reddish composition that indicates the presence of clay and rounded clasts, transported and redeposited by the rivers and wind. The detailed description of these formations can be found at Campos and Dardenne, (1997). In the Bambuí group, the erosion in the *Capacete* formation caused the emergence of sandstone

of the *Areado* group and a large portion of claystone and carbonate from the *Lagoa do Jacaré* formation (Campos and Dardenne, 1997).

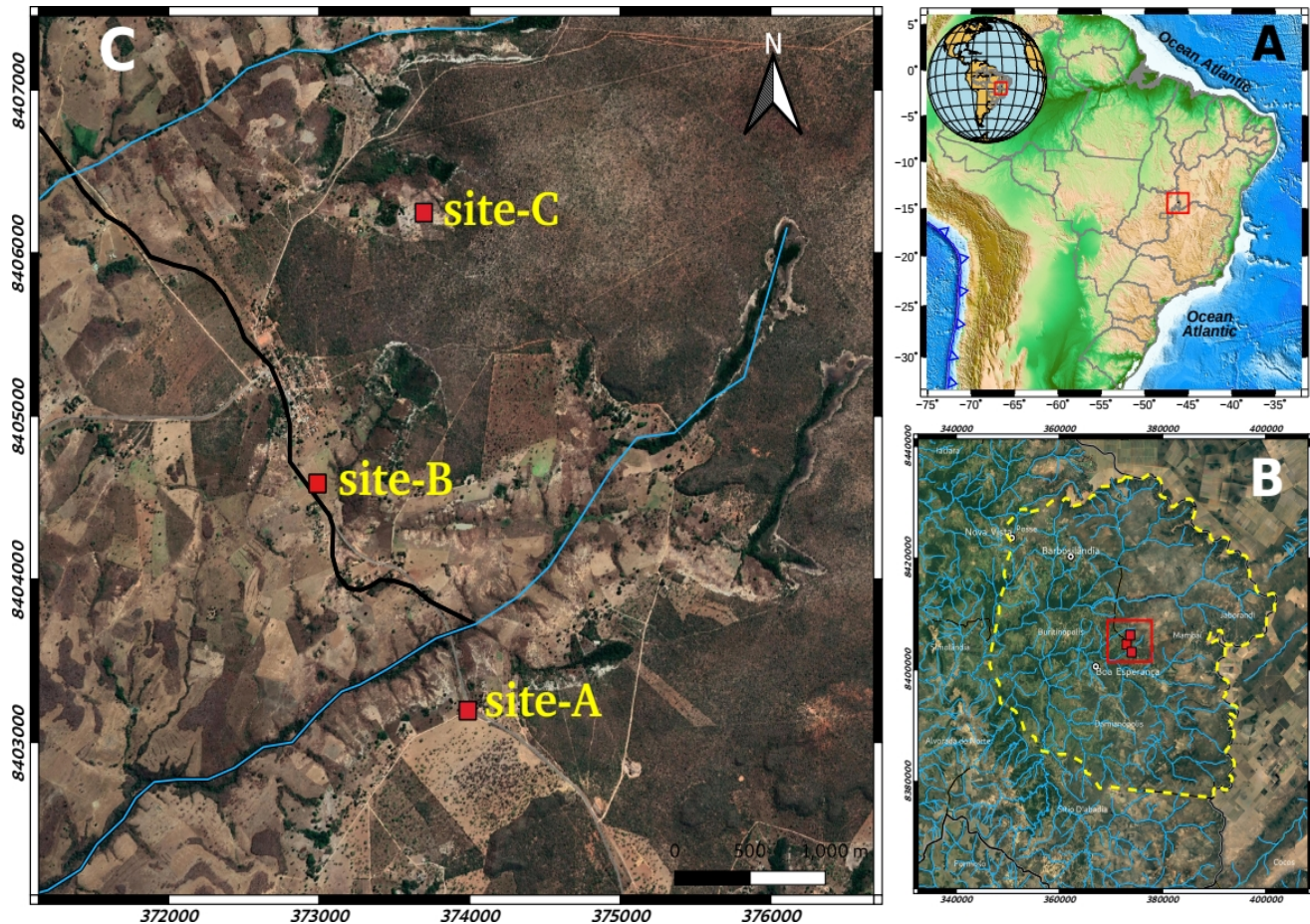


Figure 1 (A) Location of Brazil on the map of South America, (B) location of the studies area on the environmentally sensitive area of River Vermelho and (C) Locations of studied sites (A,B and C) on Tarimba cave.

The soils of the region are controlled by the stratigraphy of the site. The sandstone found in contact with the formation of the alligator pond (carbonate) which has undivided intercalations between Pelitic rocks having a large proportion of fine-grained material and with the epikarst of the carbonates (Limestone and Marlstone). In the study area, the soils are divided into: a) Arenosols at the tops connected to the presence of sandstone, with more than 90% of sand in its composition, being well-drained; b) Leptsols, shallow soils that develop through Lutites that have around 50% clay in their composition, with a high incidence of runoff production; and, c) Chernosolos, irregular soils of varying

depth that develop from the weathering and dissolution of the Limestone. Its composition depends on the degree of impurity of the Limestone and the percentage of clay can vary widely, from 4 to 30%. They are usually well-drained.

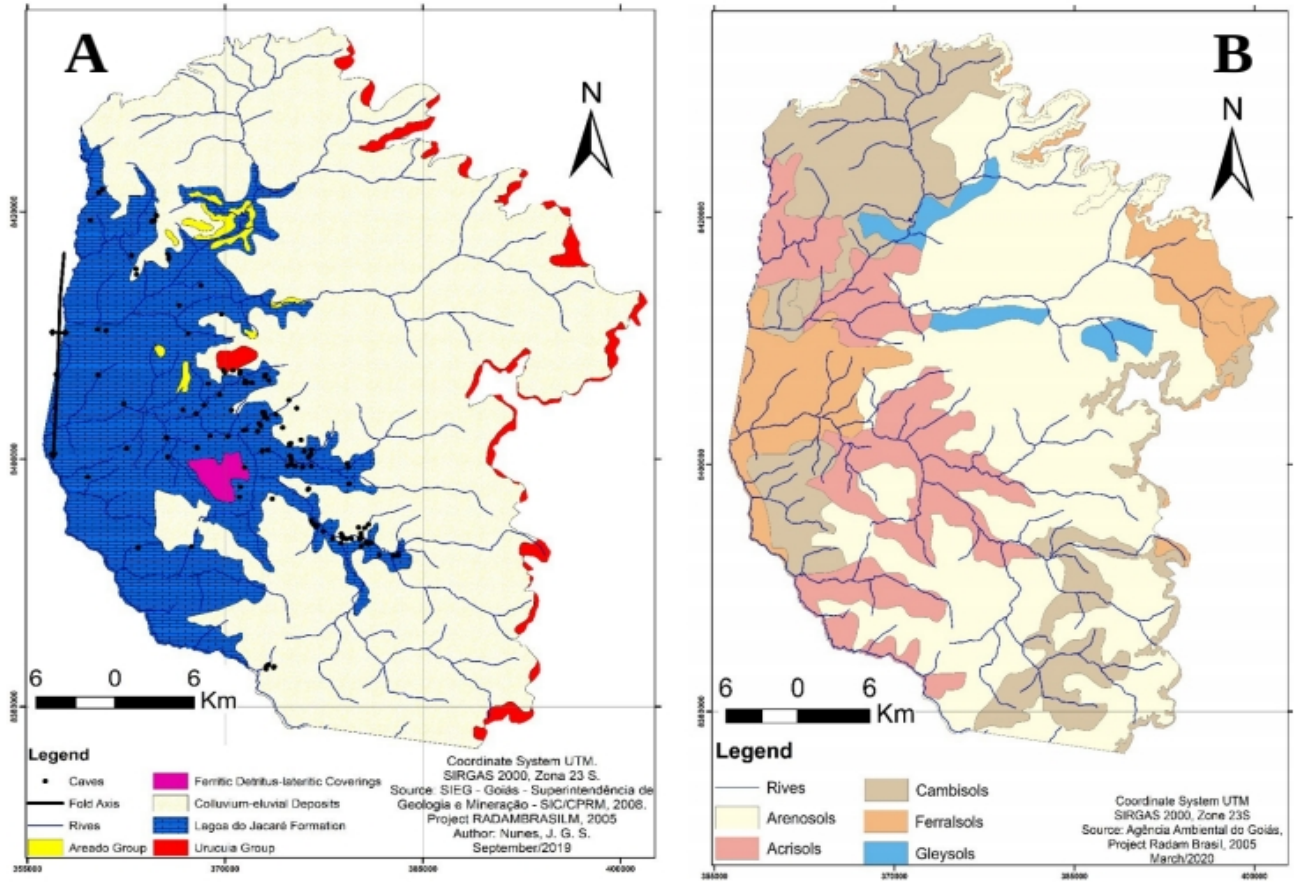


Figure 2 A) Geological and B) soil maps of the environmentally sensitive area of the River Vermelho showing different geological units, surface hydrology and the presences of mapped caves and b) geological based soil classification map of the same area.

The contact between soils depends on the stratigraphic sequence. As the *Lagoa do Jacaré* formation has an undivided distribution of lithofacies like Lutites and Carbonates, at some places the sandstone may have direct contact with the epikarst (Chernosolo and Limestone). Between the highly drained sandstone and epikarst there is a presence of metric to decimetric layer of Lutite having lower permeability which provides a protective layer for the underlying karst by generating the surface runoff. The soil classification is based on the local geology as the Argisols and Oxisols in the carbonate rock domains

(>90 % sand and well-drained), while the Neosols in the Urucuia groups (Posse and Serra das Araras formation) and the Areado group (alluvial-colluvial). These soil classes of the area are shown in Figure 4b.

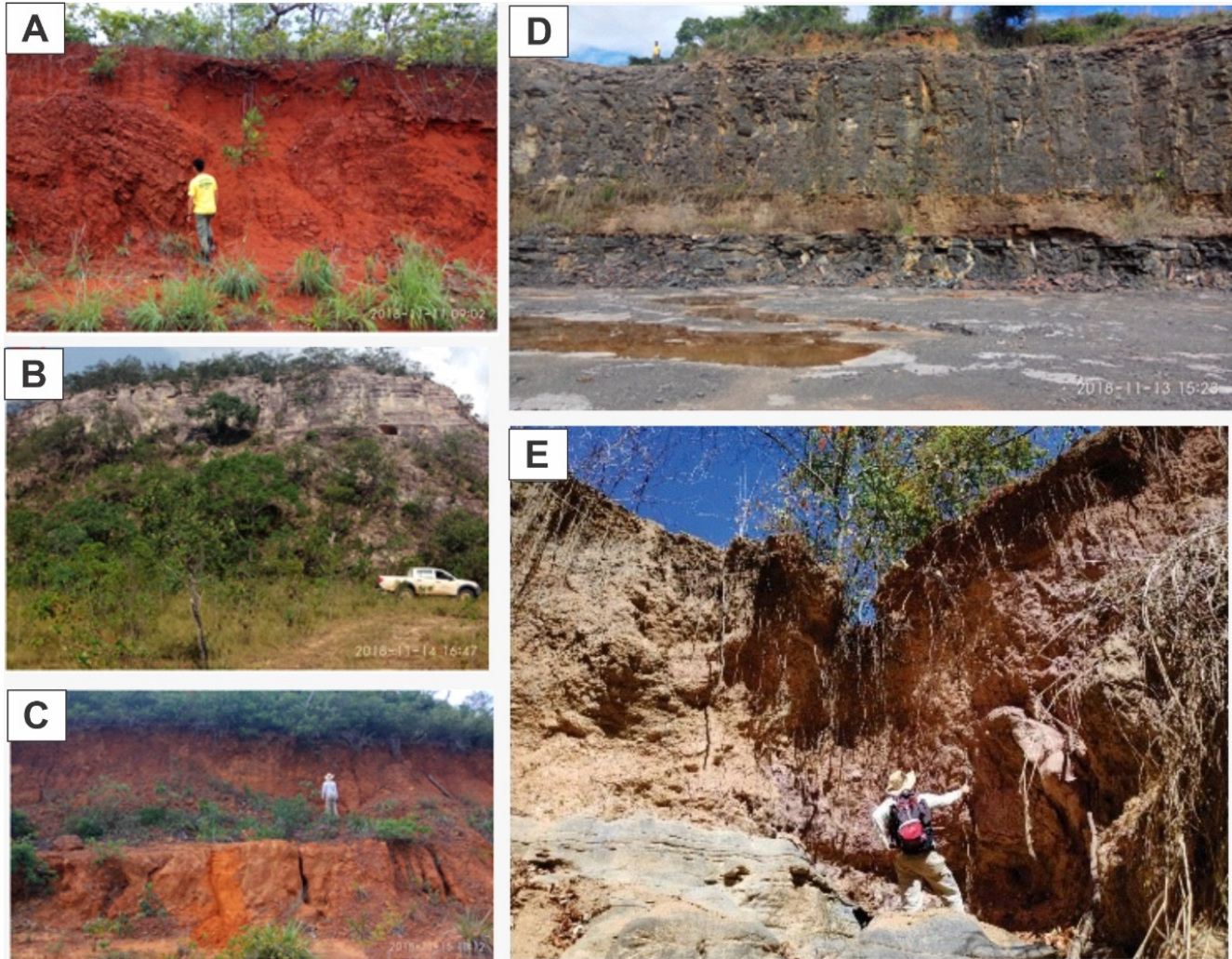


Figure 3 Photographs of different soil and rock units exposed in the area. Soil types are A) Ferrossolos and Serra das Araras Formation, B) Arenosols and Posse Formation and C) Cambisols and Areal group; D) Acrisols and Claystone and Lagoa do Jacaré formation.

In the study area, the soils are divided into: a) arenosols at the tops connected to the presence of sandstone, with more than 90% of sand in its composition, being well-drained; b) Leptpsols, shallow soils that develop through Lutites that have around 50% clay in their composition, with a high incidence of runoff production; and, c) Chernosolo, irregular soils of varying depth that develop from the weathering

and dissolution of the Limestone. Its composition depends on the degree of impurity in Limestone and the percentage of clay, which varies greatly, from 4 to 30%. This soil type is also well-drained. The contact between different types of soils depends on the stratigraphic sequence. As the *Lagoa do Jacaré* formation has an undivided distribution of lithofacies like Lutites and Carbonate, sometimes the sandstone may be in direct contact with the epikarst (Chernosolo and Limestone). Most of the time, however, between the highly drained sandstone and the epikarst there is a metric to a decimetric layer of Lutite that generates runoff, waterproofing the karst. In cases where sandstone and carbonate rocks are in contact, there is a risk of infiltration and contamination of karst aquifers. However, when the carbonates are covered by Lutites there is a high incidence of runoff and so the sediment production, which are transported on the slope and reach the karst system after reaching the pathways to the caves in dolines, causing great impacts to the underground hydrological system.

2. Materials and Methods

2.2 Electrical Resistivity Tomography (ERT)

In ERT method, a potential difference is measured in response to the injection of a known amount of electrical current in the earth. Different earth materials have different resistance to the passage of current because of the variation in the degree of fractures, material types and degree of saturation. Both the injection of current and the detection of potential difference are carried out using four metal electrodes, current and potential, respectively (Hussain et al. 2020A, Hussain et al. 2020B). The way in which these electrodes are configured has a direct influence on the results, and there are three adopted ways in which electrodes are configured as i) vertical electrical sounding (VES), ii) profiling and iii) electrical tomography. VES is applied where the target is the determination of physical property of the subsurface with depth only (1D). VES has a greater depth of penetration and spread length (Strelec et al. 2017). Profiling is used for the estimation of both vertical and lateral changes in the subsurface, as is the case with karst studies. Under these conditions, 2D and 3D images are obtained by the resistivity

tomographic techniques. ERT has been proved effective in karst studies such as their structures, soil cover and cavity geometry and more importantly the characterization of cavity sediments, study of which is crucial for the speleology, the groundwater vulnerability and the associated geologic hazards. So, the method can be used as ground truth for the results accuracy assessment of the other applied geophysical methods (GPR and VLFEM).

2.3 Ground Penetrating Radar (GPR)

Among different geophysical methods (including resistivity and seismic refraction) Ground Penetrating Radar (GPR) has the finest resolution - depending on the antenna used and the soil types in the area. Here, subsurface image is obtained by passing electromagnetic waves of various frequencies through the ground. These energies are radiated from the antenna, which either absorbed or reflected depending on the underlying material properties such as fractures, caves, moisture and clay contents. The energy reflected by the surface discontinuities is detected by a receiver, which helps in subsurface image construction. The amplitude of radar pulse is an essential factor because it can carry information about the ground. After time to depth conversion, these amplitudes help in mapping the subsurface discontinuities. The higher the contrast at the interface of these discontinuities, the higher the amplitudes are, and vice versa. The detailed description of its applicability can be found (Čeru et al. 2018). A detailed description of this method and its application of cave studies is presented elsewhere (e.g. Xavier and Medeiros, 2006; dos Reis Jr et al. 2014; Fernandes et al. 2015; Jin-long et al. 2018; Conti et al. 2019). Radar stratigraphy was used in the for the interpretation of reflectors. Various radar reflection typologies which may be caused by lithological and soil variations such as differences in grain compositions (e.g. presence of iron oxides), size, orientation, packing and shape of grains, changes in grain-size parameters, degree of sorting and porosity of the sediments are analyzed (Lejzerowicz et al. 2018).

2.4 Very Low-Frequency Electromagnetic (VLFEM)

In this semi-passive induction method, primary field originated from distant high power vertical transmitter (marine communications) is used. The signals from this transmitter at a frequency band of 15-30 kHz can travel a long distance and have potential geophysical implications even in areas of thousands of km away from transmitters (Sungkono et al. 2014; Singh and Sharma, 2016). The horizontality of the primary field makes it an ideal choice for the investigations of vertical and dipping subsurface structures such as caves. The signals from transmitter generate a primary field while traveling between earth surface and ionosphere. This primary field generated a secondary field which differs in the phase when coming in contact with a conductor (water-filled cave or fracture). Thus, VLF measures both primary and secondary fields and detects the conductive structures and geological contacts like altered zones, faults, and conductive caves (McNeill and Labson, 1990; Guerin et al., 1994) at an approximate depth of 30m (Fraser, 1969).

2.5 Data acquisition and processing

The GPR survey was performed using a georadar device GPR GSSI SIR 3000, with 400MHz Antenna, Control Unity and Rugged Survey Car, in order to obtain a proper resolution. One profile of 180 m length near the Tarimba was conducted, at the location shown in Figure 1. The electrical resistivity data were acquired three profiles at different locations (Figure 1). A total of 72 electrodes were used for injecting current in the subsurface as well as to measure the potential difference developed in response to these currents. The length of each profile was taken as 360 meters with an electrodes spacing of 5m. Three ERT profiles were taken at two different sites. The first was a road (APA01), and the second and third were taken near the Tarimba cave (APA02). The profiles at Tarimba passes parallel and perpendicular to the cave, as shown in Figure 1. In the present work, VLFEM data were collected along a single profile of about 600 m length at the pavement. This site was chosen because of a lesser level of noise and easy accessibility (Figure 1). The receiver used in this study is T-VLF unit (IRIS- Instruments, 1993), which can apply automatic filters together with the

digital stacking that can improve the signal to noise ratio. The survey was carried out in the tilt (magnetic) mode.

In the first stage, the electrical resistivity data of each line was opened in Prosyscal II software in order to identify the anomalies and error in the data. Those resistivity values, which are quite high, were manually removed from the data. After the initial data editing, the RESIS2DINV of Geotomo Software (Loke, 2004) was used for the inversion of data where apparent resistivity values were used for the generation of a best-fit earth model. Here cell-based calculation was carried out by applying smoothness-constrained least-squares inversion method (Sasaki, 1992), where a search for an ideal subsurface resistivity best-fit model was made (Colangelo et al., 2008). In this method, the subsurface is divided into rectangular blocks, each representing a single measuring point (Lapenna et al., 2005). The root means square error (RMS) provides the discrepancy between the measured and the calculated values.

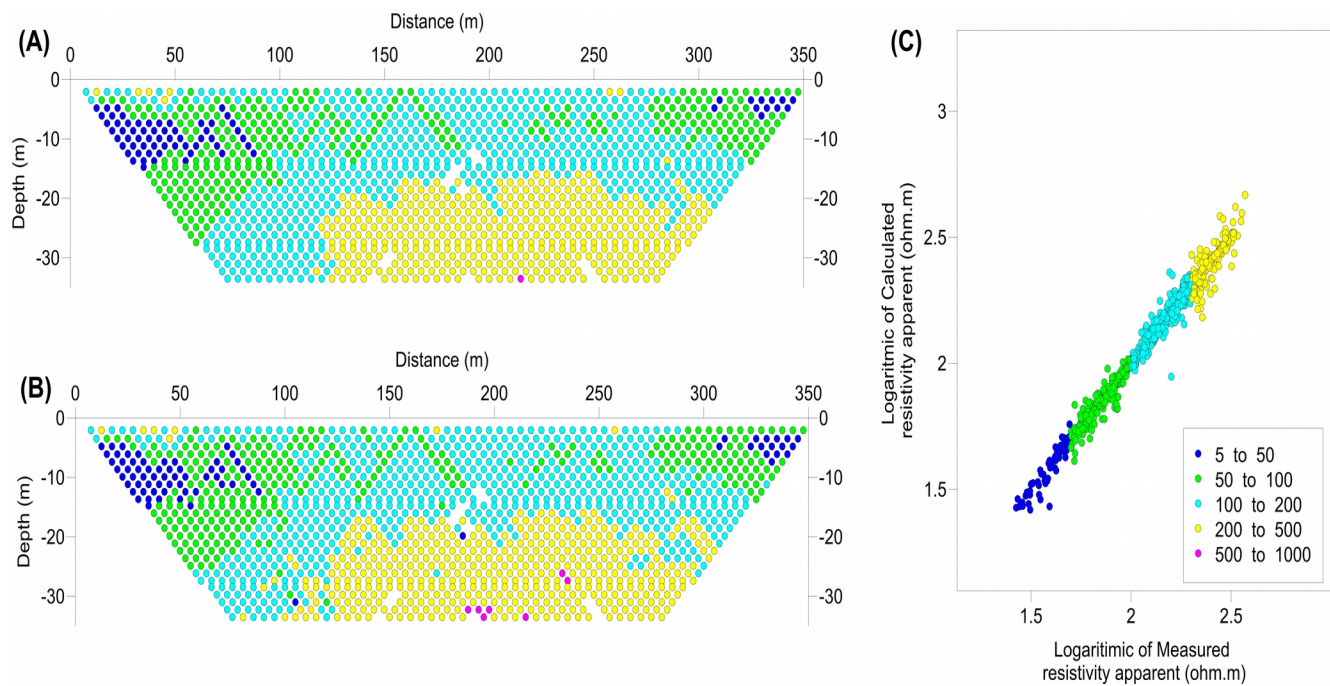


Figure 4. A) Observed and B) measured apparent resistivity of profile APA01. C) logarithm of the apparent vs calculated values of APA01.

For GPR data processing and visualization, ReflexW (Sandmeier, Inc.) was used where the following necessary processing steps were employed: (i) static correction for the time zero setting; (ii) 1D Dewow filter with a pulse of 2.5ns period is applied to remove noise induced by the electromagnetic induction of the equipment (electronic noise); (iii) removing the header which was inserted prior to the acquisition of data; iv) applying a combined gain filter (four linear and two exponential) in order to compensate abrupt changes in signal amplitude; (v) application of 2D filter for the removal of coherent noise which resulted in the areas where GPR signal attenuate quickly such as Chernosolos. The value used for the filter was 100 trace; vi) filter application 1D type bandpass frequency for removing random noise of high frequency, the cutting intervals of 172, 258, 688 and 828 MHz were used; vii) collapse of diffraction with the migration of routine type diffraction stack. The values used were verified hyperbolas observed in the sandy soil at the beginning of the profile. Width 50 trace and speed of 0.1 m/s. viii) subsequently, for the trace envelope (instantaneous amplitude) generation, the filter was applied without changing these parameters since the same applies to the Hilbert transform data. ix) In the end, topography of the profile was inserted.

For the subsurface characterization using VLF data, a quantitative approach was adopted, which included examining and plotting Karous-Hjelt transform (Karous and Hjelt, 1983). It transforms raw (unfiltered) data to current density Karous-Hjelt, the current density pseudo-sections of the VLFEM data, were produced in KHFFILT computer program (Pirttijarvi, 2004). The Fraser filter uses real and imaginary parts depict a single positive, and both positive and negative peaks above a conductor, respectively. The imaginary part is used for the quality assessment of the conductor, however, in the present study, the only real part is used for the pseudo-section of relative apparent current density variation with depth. In this way, on real data the areas of positive anomalies show zones of groundwater (Ariyo et al. 2009). From the pictorial presentation of the depths of various current densities, the subsurface geological features are delineated. The pseudo-section is shown as color codes with conductivity increasing from negative to positive.

Further details can be accessed at Jamal and Singh (2018). The positive and negative values of current values are representative of conductive and resistive bodies in the subsurface, respectively. Hence, the sub-surface features of high conductivity are identified on the VLF profile as possible fracture/weathered carbonate rocks zones and sinkholes filled with conductive materials.

3. Results and discussions

3.1 Electrical Resistivity Tomography (ERT)

The results of two resistivity profiles taken in the area near a road and the entrance of the Tarimba cave are shown in Figures 4 and Figure 6. In these areas, ERT was successfully able to mark the presence of fracture, sinkholes and different soil types providing a different degree of geogenic protection to the cave environment. The possible stratigraphic picture revealed the presence of a very thick soil layer, followed by a layer of the claystone. Below the claystone are the weathered carbonate rocks of the Bumbai group. It is interesting to note that resistivity section of profile APA01 the subsurface material showed a pattern which indicates the absence of karst features at shallow depth in the area. The carbonate rocks were found at a depth of 30m. The upper layer showed clay with a high degree of moisture. This moisture content decreases with depth. Below the clay, there is an interface of claystone. It is clear from the results (Figure 5) that Tarimba cave does not pass through that site. At the beginning of the profile, a fracture-filled with sediments with varying degree of moisture and clay contents can be interpreted. There is a high probability of the presence of the sinkhole. This was also confirmed by the site visits, and an active karst structure in the nearby area is presented in the Figure 6. This edge of the profile lies near the area where the Tarimba cave passed near the surface, having an important high use for the transportation of Limestone for the cement industry. At the middle of the profile (~160m) a vein of intermediate resistivity can be seen, which might be attributed to the presence of coarse-grained material. This structure has a very important impact on karst. It can provide pathways to the precipitation for infiltration that can lead the dissolution of the below karst. Therefore their study is crucial in the safety management of the important structures such as road in

this case. Another important aspect is the fast motion of the contaminants in the caves, that can cause possible damage to the underlying karst habitat. It can be assumed that there may be an active karst structure at the start of this profile whose geometry cannot be delineated because of the shorter length of the profile. This structure may also recreate other geological hazards in the adjoining areas. Therefore, for the protection of the nearby population and the health of the roads, further detailed investigations are recommended.

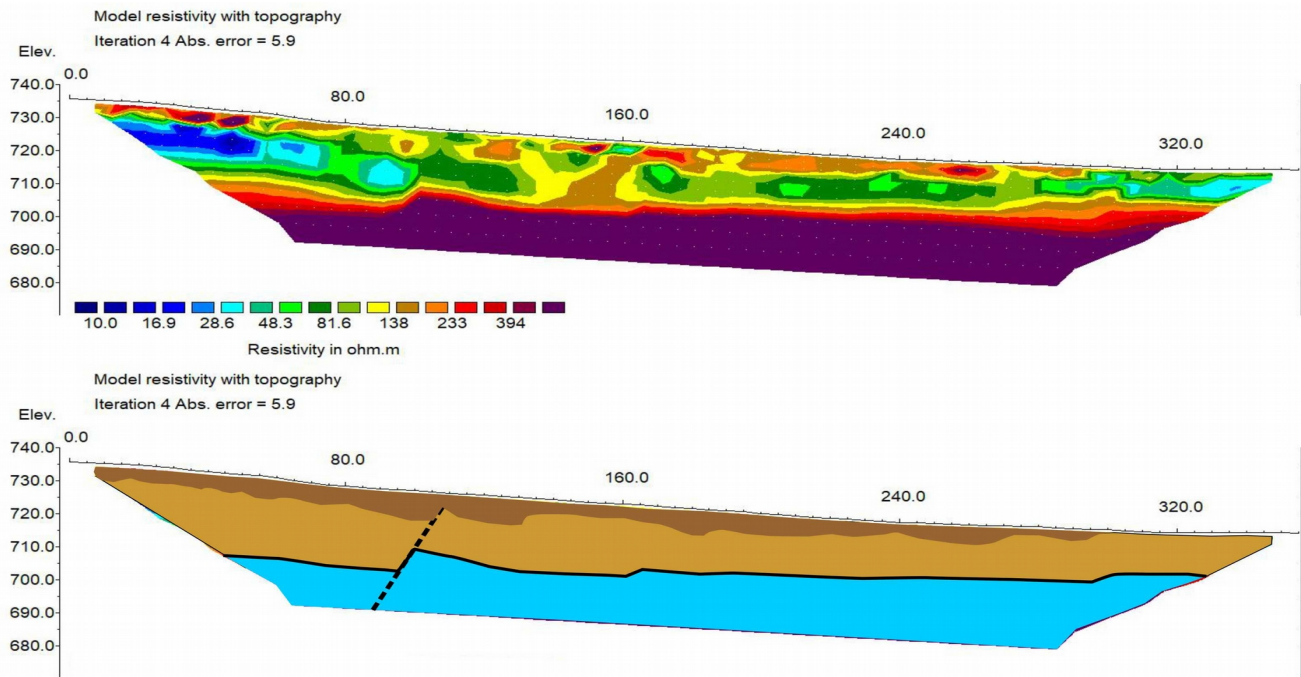


Figure 5 The modeled earth resistivity pseudo-sections for APA-01 ERT profile at the Site-A (road). Color bar presents resistivity values in ohm.m. Below is the interpreted resistivity values in the form of different structure and stratigraphy. The black dotted line marks the presence of a possible fracture.



Figure 6. Site photographs taken near the ERT profiles. (A-C) of the nearby APA01 sinkholes and an erosion site. D) surficial opening of the Tarimba cave lies near APA02 profile.

The peculiarity of the APA02 profile is, it passes through the mapped galleries and the sinkholes both open and filled on the Tarimba cave. At about 80 m it shows a low resistivity passage to the cave, that is a possible sinkhole filled with sediments with a considerable amount of moisture. Next to it is a high resistivity zone indicates the carbonate rock. This can also be seen in the site photographs (Figure 6). At the middle of the profile, a filled sinkhole was found, which may present geological hazards and groundwater contamination site. This area is sensitive because of the presence of the cave openings. At the middle of the profile APA-02, a high resistivity material was encountered, which can be linked with sinkhole filled with dry and coarse-grained material (Figure 7). It can be assumed that water entered through the fracture and traveled downward, which is shown as a low resistivity zone at the center of the profile. At the right side of

the profile, sandstone with various degree of moisture was found. It is interesting to note that at the middle of the profile, a low comparative resistivity was found which may provide a path to water flow that dissolve the carbonate rocks. Its relationship with the karst is also evident from the weathered carbonate around this low resistivity central zone. In this way, new sinkholes may emerge. These are areas which should be avoided for any future construction projects. This understructure is also crucial for the environmental and managerial planning for the cave environment of the area.

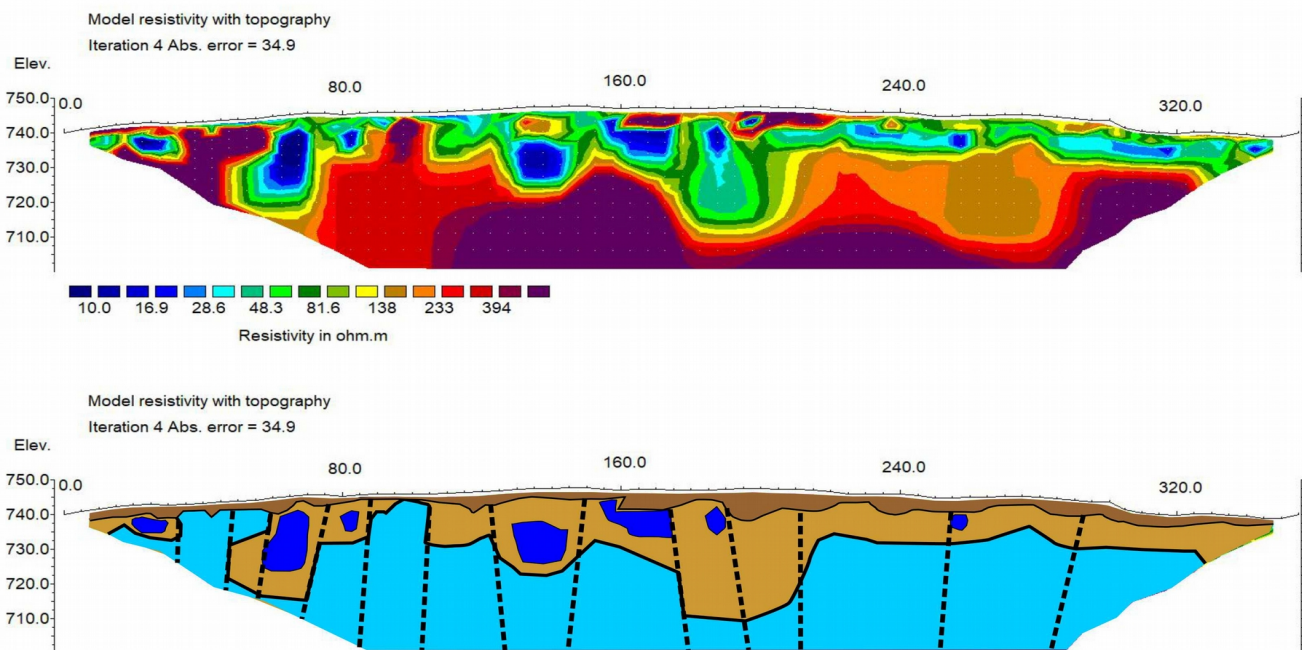


Figure 7 a) The modeled resistivity pseudo-sections for APA-02 ERT (Tarimba cave) profile. Color bar presents resistivity values in ohm.m. b) lithosection based on inverted resistivity values.

A three-layered stratigraphy similar to the APA01 is also found here: a thick soil layer, then claystone and the carbonate rocks. However, the depth to the carbonate rocks is very variable, which indicates a higher degree of karstification at this location. The carbonate rocks can be seen as having varying degree of weathering; this weathering in the carbonate can also provide a potential pathway to the surficial contaminants to the underground hydrological system. The undulation topography of the underlying carbonate rock can influence the groundwater flows as well. In this way, in the depressions created by the dissolved carbonate can possibly provide a longer time for the groundwater to stay and

thus had greater chances of the reaching of the contaminant to the groundwater or underlying cave. The stagnant water can also enhance the dissolution potential leading to the development of epikarst features i.e. geological hazard. The weathered carbonate rocks can be an essential aspect of groundwater development in the region (Hasan et al. 2018). The lithological contact between different rock and soil types can also influence the infiltration conditions and associated hazards. The sites of the contacts between the sandstone and carbonate are in the potential permeable paths that can increase the infiltration of water with contaminates to the karst aquifers. Different soil and rock contacts are shown in Figure 6, 7. In this way, weathered carbonate also provides a conducive environment to the groundwater, increasing the vulnerability of the area. In short, all delineated lithological units on electrical cross-section have an essential role in the vulnerability assessment and geological hazard studies.

3.2 Ground Penetrating Radar (GPR)

Using the GPR method, a profile was taken outside the cave at a location where various lithologies are present. Figure 8 shows the vertical cross-section of the subsurface of the area obtained from the reflection of electromagnetic waves. Three georadar amplitude typologies are delineated (Figure 8). The amplitude of the electromagnetic wave is divided into three categories as high, intermediate and low. At the beginning of the profile, there is sandstone through which the electromagnetic wave can pass easily. As a result, high amplitude reflection was observed on the 2D cross-section obtained (Figure 8). At the middle of the profile, material absorbed the electromagnetic waves and gave rise to low amplitude wiggles. This high attenuation medium is attributed to the presence of Litolic Neosol. At the end of the profile, there are patches of Limestone, the presence of which caused some radar wiggles of high amplitude to appear on the cross-section. However, it is interesting to note that in the middle portion, some wavy wiggles were observed, as these were noisy events created by the passing of four-

wheeler vehicle used for the GPR data acquisition. This phenomenon occurs because GPR antenna does not touch the soil, which may cause some noisy wiggles on the GPR cross-section.

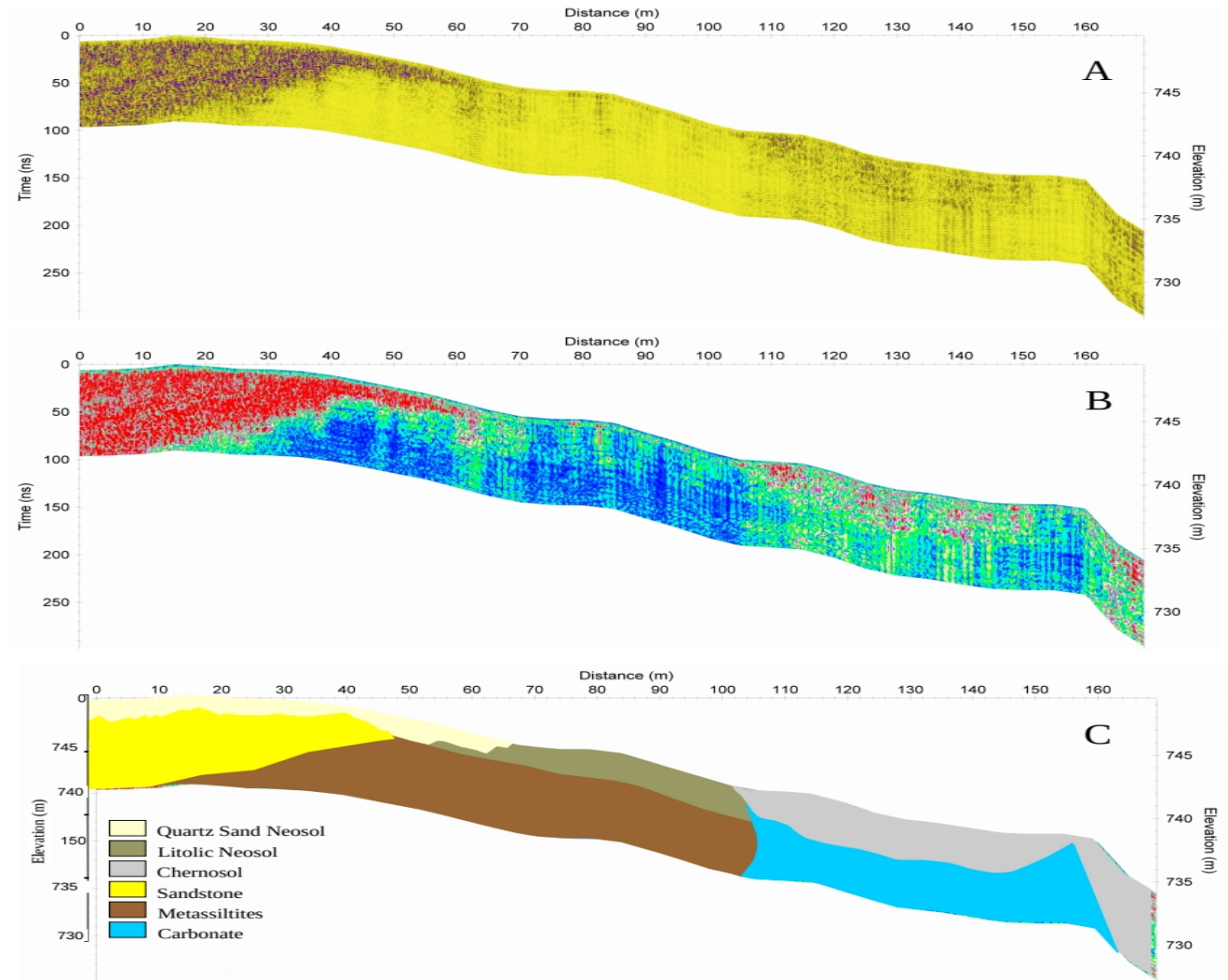


Figure 8. a) GPR results, b) lithological cross-section obtained from GPR amplitude. Different soil types as well a sharp contact between the carbonate of Bambui group and soil is evident. Prominent reflections are zoomed in Figure 8.

The various radar typologies based on the amplitude and geometries of the reflectors such as continuous, discontinuous, linear and inclined have also been found (Figure 9). Different radar typologies are used for the delineation of different subsurface structures that can possibly influence the groundwater vulnerability. The features associated with the weathered carbonates have also been found. They are presented on the radar images and continuous medium amplitude reflectors which can

be associated as potential water flow pathways. These are very important hydrogeological features the presence of which can increase the vulnerability of the sites. They may also be considered as the potential recharge sites for the underlying aquifer.

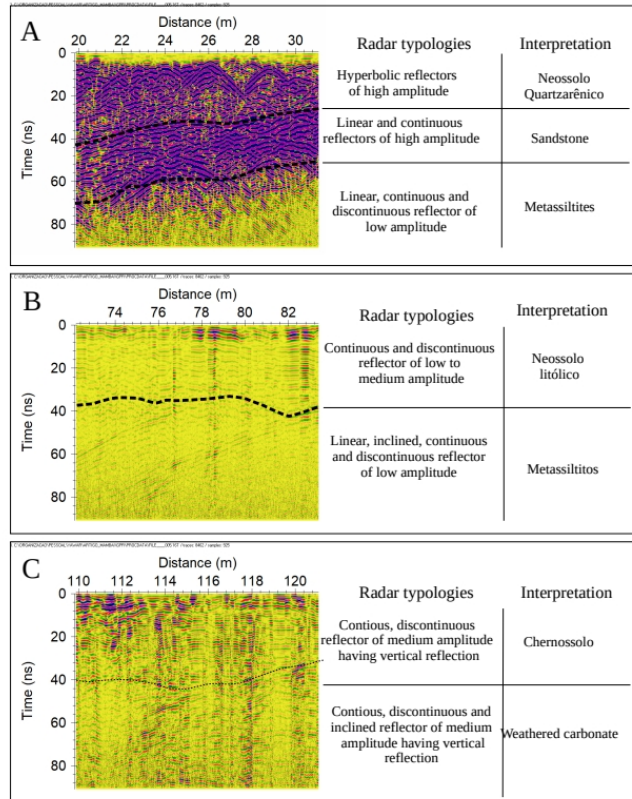


Figure 9. The prominent radar typologies. Zoomed images of different radar images along with the possible lithofacies shown is Figure 8. A) high amplitude reflections associated with sandstone, B) low energy reflections may indicate the presence of attenuative material possibly Neosolo and Metassilites and C) intermediate amplitude reflections (energy) indicates the presence of Chermssolo.

These different soil and rock types have their own significant role in the infiltration conditions that lead to the aquifer vulnerability, generation of surface runoff and the aquifer recharge. The presence soil which which has greater proportions of fine-grained material or clay proportions, low permeability can potentially inhibit the infiltration, generate the larger amount of surface runoff with sediments load that can enter the cave. This large sediment influx in the cave can also have negative impacts on the cave habitat. These specific soil and rock types can also significantly reduce

groundwater recharge. However, when the carbonates are covered by Lutites in the study area, there is a high chance of runoff and sediment production. However, previous studies found higher clay content, and rich iron/aluminium oxides/hydroxides in sediments can affect the GPR depth penetration (Čeru et al. 2018). The reverse is true for the soil type with greater proportions of the coarse grain material, which can increase the infiltration, thus lower runoff and sediments load. This soil type is also conducive for the greater depth penetration of GPR. This relation of radar wave amplitude and grain size, changes in porosity, changes in the coefficient of reflectivity has been extensively studied (Guillemoteau et al. 2012; Lejzerowicz et al. 2018; Akinsunmad et al. 2019).

3.3 Very Low-Frequency Electromagnetic (VLFEM)

With apparent current density cross-section plots, it is possible to qualitatively discriminate between conductive and resistive structures where a high positive value corresponds to conductive subsurface structure, and low negative values are related to resistive one. Different features of varying degree of conductivity coinciding with points already identified on the profiles (as fractures or geological features) were delineated on the section. Some of these conductive materials are linear, while others are dipping features (Ndatuwong and Yadav, 2014). The apparent current density cross-section of the profile VLFEM (Figure 9) revealed the presence of a significant high conductive anomaly at about 150m from the start of the profile. This anomaly coincided with the existing buried cave in the study area at a previously known location. Furthermore, three high current density zones at about 40 m and 320 m along the profile (Figure 8) can also be inferred as indications of the potential subsurface caves or fractured aquifer as evident from the various groundwater developments in the adjoining areas. There is a dipping conductive structure which can be a potential zone of groundwater development. A similar high current density (like a vein shape) has been observed in many previous studies. It is quite interesting to note that throughout the entire length of the profile, structures of intermediate resistivity values can be seen. These indicate the possible presence of the weathered or

dissolved carbonate structures. This may also indicate the presence of groundwater as there were already many installed water pump in the area. These structures are also important for the assessment of geological hazards impacting the people living nearby as well as for the cave habitat. As described in section 3.1, such conductive structures can also increase the probability of groundwater contamination by anthropogenic contaminants. In short, VLFEM has appeared a non-invasive reconnaissance tool for the area which guides the future details studies.

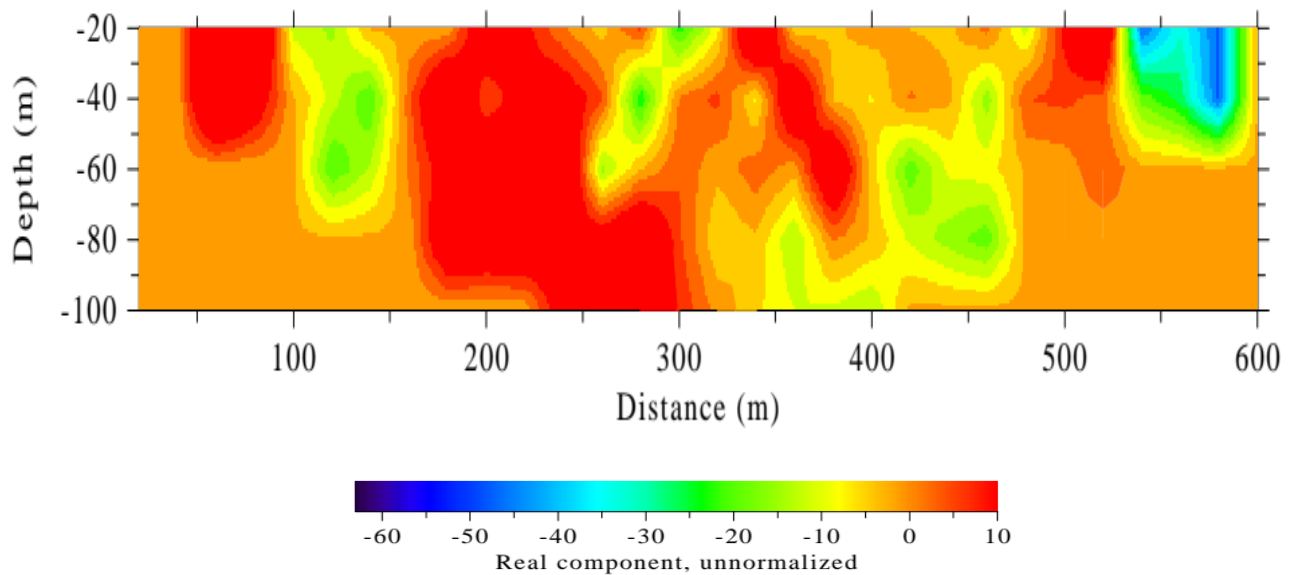


Figure 10. Karous-Hjelt current density pseudo-section showing inferred / potential conductive and resistive structures along VLFEM profile. Current density scale is arbitrary color codes with with conductivity increasing from negative to positive. The high positive value constitutes the conductive sub-surface and low negative value represents a resistive subsurface.

In the case of covered karst (of Mambai), the properties of soil and the degree of karstification that are related to the development of karst features such as sinkholes, conduits and degree of weathering affect the underlying groundwater flow system. This leads to the vulnerability of fauna and flora of the caves, i.e. a threat to the cave habitat. Under these conditions, the thickness of the soil and the degree of karstification can protect the system. A high vulnerability is associated with the thinner soil, coarse-grained soil, and lesser degree of karstification. The applied methods have their limits and advantages

in the characterization of the karst area, such as Mambai. The comparative remarks of the methods can be made based on the data acquisition, processing as well as interpretation, spatial resolution and depth of the penetration. In terms of depth of penetration and data acquisition and processing, VLFEM should be the top priority. However, results are not so reliable because of the noise levels created by the proximity to the electrical cables, metal bars etc. The other appropriate choice to achieve considerable high resolution at greater depth is ERT. In the present study, the ERT was able to delineate very important subsurface hydrogeological and hazardous subsurface conditions. The cavities, collapsed sinkhole, the geometries of the filled karst structures and the well-defined site stratigraphy. Georadar was better able to resolve soil types, their contacts and the pathways for water infiltration at a finer resolution as compared to other used methods. However, it suffers from a severe limitation, the lower depth of penetration.

4. Conclusions

The research demonstrated that the geophysical methods used in this study (GPR, ERT and VLFEM) have varying potentials for the investigation of the karst system. Each method showed different capabilities in terms of detecting possible cavities, potential sinkholes or paths for water infiltration that have a direct impact on the vulnerability of cave water reservoir.

The resistivity section of ERT, which was obtained at the road site, did not show the presence of a cave or groundwater. However, the inverted resistivity sections at the cave site showed the presence of cave and fractures, highlighting the need for further investigation for the groundwater prospecting.

Based on the GPR profiles, it was possible to distinguish between different rock units. In this way, the GPR has proved an attractive choice for the site characterization in the selected karst areas. However, because of the high attentive soil cover, it was not possible to obtain information about the presence of caves using electromagnetic waves. Therefore, GPR was found to be not suitable for the investigation of deeper karst structures in the covered karst area having comosolo.

Qualitative interpretation of VLF-EM profiles using different linear filtering such as Fraser and Karous–Hjelt showed a subsurface low resistivity zones which lie in the vicinity of the low apparent resistivity value observed in the gradient profiling. On VLF profile, conducting bodies were observed which might be linked with the presence of subsurface cavities (karst features) with a large amount of moisture.

Author Contributions: Conceptualization, Y.H.; methodology, Y.H.; software, Y.H. and W.B.; validation, Y.H.; formal analysis, Y.H.; investigation, Y.H.; data curation, Y.H.; writing—original draft preparation, Y.H.; writing—review and editing, Y.H., and O.H; visualization, X.X.; supervision, R.A.; project administration, R.A.; funding acquisition, R.A. All authors have read and agreed to the published version of the manuscript.

Conflicts of Interest: The authors declare no conflict of interest.

Reference

- Abbas, A. M., Khalil, M. A., Massoud, U., Santos, F. M., Mesbah, H. A., Lethy, A., ... & Ragab, E. S. A. (2012). The implementation of multi-task geophysical survey to locate Cleopatra tomb at tap-Osiris Magna, Borg El-Arab, Alexandria, Egypt “phase II”. *NRIAG Journal of Astronomy and Geophysics*, 1(1), 1-11.
- Abidi, A., Demehati, A., Banouni, H., & El Qandil, M. (2018). The Importance of Underground Cavities Detection in the Choice of Constructible Areas: Case of the Agglomeration of Fez (Morocco).
- Akinsunmade, A., Tomecka-Suchoń, S., & Pysz, P. (2019). Correlation between agrotechnical properties of selected soil types and corresponding GPR response. *Acta Geophysica*, 67(6), 1913-1919.

- Al-Tarazi, E., J. Abu Rajab, A. Al-Naqa, and M. El-Waheidi. "Detecting leachate plumes and groundwater pollution at Ruseifa municipal landfill utilizing VLF-EM method." *Journal of Applied Geophysics* 65, no. 3-4 (2008): 121-131.
- Ammar, A. I., & Kruse, S. E. (2016). Resistivity soundings and VLF profiles for siting groundwater wells in a fractured basement aquifer in the Arabian Shield, Saudi Arabia. *Journal of African Earth Sciences*, 116, 56-67.
- Andreo, B., Ravbar, N., & Vías, J. M. (2009). Source vulnerability mapping in carbonate (karst) aquifers by extension of the COP method: application to pilot sites. *Hydrogeology Journal*, 17(3), 749-758,
- Argentieri, A., Carluccio, R., Cecchini, F., Chiappini, M., Ciotoli, G., De Ritis, R., ... & Materni, V. (2015). Early stage sinkhole formation in the Acque Albule basin of central Italy from geophysical and geochemical observations. *Engineering geology*, 191, 36-47.
- Ariyo, S. O., Adeyemi, G. O., & Oyebamiji, A. O. (2009). Electromagnetic Vlf survey for groundwater development in a contact terrain; a case study of Ishara-remo, Southwestern Nigeria. *Journal of Applied Sciences Research*, 5(9), 1239-1246.
- Auler, A., & Farrant, A. R. (1996). A brief introduction to karst and caves in Brazil. *Proceedings of the University of Bristol Speleological Society*, 20(3), 187-200.
- Auler, A. S. (2002). Karst areas in Brazil and the potential for major caves-an overview. *Bol. Soc. Venezolana Espel*, 36, 29-35.
- Bishop, I., Styles, P., Emsley, S. J., & Ferguson, N. S. (1997). The detection of cavities using the microgravity technique: case histories from mining and karstic environments. Geological Society, London, *Engineering Geology Special Publications*, 12(1), 153-166.
- Bosch, F. P., & Müller, I. (2001). Continuous gradient VLF measurements: a new possibility for high resolution mapping of karst structures. *First Break*, 19(6).

Čeru, T., Gosar, A., & Šegina, E. (2017, June). Application of Ground penetrating radar for investigating sediment-filled surface karst features (Krak Island, Croatia). In 2017 9th International Workshop on Advanced Ground Penetrating Radar (IWAGPR) (pp. 1-6). IEEE.

Čeru, T., Dolenc, M., & Gosar, A. (2018). Application of Ground Penetrating Radar Supported by Mineralogical-Geochemical Methods for Mapping Unroofed Cave Sediments. *Remote Sensing*, 10(4), 639.

Chalikakis, K., Plagnes, V., Guerin, R., Valois, R., & Bosch, F. P. (2011). Contribution of geophysical methods to karst-system exploration: an overview. *Hydrogeology Journal*, 19(6), 1169.

Colangelo, G., Lapenna, V., Loperte, A., Perrone, A., & Telesca, L. (2008). 2D electrical resistivity tomographies for investigating recent activation landslides in Basilicata Region (Southern Italy). *Annals of Geophysics*, 51(1), 275-285.

Conti, I. M., de Castro, D. L., Bezerra, F. H., & Cazarin, C. L. (2019). Porosity estimation and geometric characterization of fractured and karstified carbonate rocks using GPR data in the Salitre Formation, Brazil. *Pure and Applied Geophysics*, 176(4), 1673-1689.

Daly, D., Dassargues, A., Drew, D., Dunne, S., Goldscheider, N., Neale, S., ... & Zwahlen, F. (2002). Main concepts of the "European approach" to karst-groundwater-vulnerability assessment and mapping. *Hydrogeology Journal*, 10(2), 340-345.

de Queiroz Salles, L., Galvão, P., Leal, L. R. B., de Araujo Pereira, R. G. F., da Purificação, C. G. C., & Laureano, F. V. (2018). Evaluation of susceptibility for terrain collapse and subsidence in karst areas, municipality of Iraquara, Chapada Diamantina (BA), Brazil. *Environmental Earth Sciences*, 77(16), 593.

de Souza MARTINELLI R, CALVO EM, LOBO HAS (2015) Exploration and mapping of dores – Tarimba – Pasto De Vacas Cave System (MAMBAÍ, Goiás, Brasil) in AN AIS do 33o Congresso

Brasileiro de Espeleologia Eldorado SP, 15-19 de julho de 2015 – Sociedade Brasileira de Espeleologia.

dos Reis Jr, J. A., de Castro, D. L., de Jesus, T. E. S., & Lima Filho, F. P. (2014). Characterization of collapsed paleocave systems using GPR attributes. *Journal of Applied Geophysics*, 103, 43-56.

dos Santos, E. S., Silva, R. W., & Sampaio, E. E. (2012). Analysis of the risk of karst collapse in Lapão, Bahia, Brazil. *Exploration Geophysics*, 43(3), 198-212.

Dourado, J. C., Malagutti Filho, W., Braga, A. C., & Nava, N. (2001). Detecção de cavidades em arenitos utilizando gravimetria, eletrorresistividade e GPR. *Revista Brasileira de Geofísica*, 19(1), 19-32.

Allred, B., Daniels, J. J., & Ehsani, M. R. (Eds.). (2008). *Handbook of agricultural geophysics*. CRC Press.

Ezersky, M. (2008). Geoelectric structure of the Ein Gedi sinkhole occurrence site at the Dead Sea shore in Israel. *Journal of Applied Geophysics*, 64(3-4), 56-69.

Fabregat, I., Gutiérrez, F., Roqué, C., Comas, X., Zarroca, M., Carbonel, D., ... & Linares, R. (2017). Reconstructing the internal structure and long-term evolution of hazardous sinkholes combining trenching, electrical resistivity imaging (ERI) and ground penetrating radar (GPR). *Geomorphology*, 285, 287-304.

Fernandes Jr, A. L., Medeiros, W. E., Bezerra, F. H., Oliveira Jr, J. G., & Cazarin, C. L. (2015). GPR investigation of karst guided by comparison with outcrop and unmanned aerial vehicle imagery. *Journal of Applied Geophysics*, 112, 268-278.

Garcia, G. P., & Grohmann, C. H. (2019). DEM-based geomorphological mapping and landforms characterization of a tropical karst environment in southeastern Brazil. *Journal of South American Earth Sciences*, 93, 14-22.

Guidry, S. A., Grasmueck, M., Carpenter, D. G., Gombos Jr, A. M., Bachtel, S. L., & Viggiano, D. A. (2007). Karst and early fracture networks in carbonates, Turks and Caicos Islands, British West Indies. *Journal of Sedimentary Research*, 77(6), 508-524.

Guillemoteau, J., Bano, M., & Dujardin, J. R. (2012). Influence of grain size, shape and compaction on georadar waves: examples of aeolian dunes. *Geophysical Journal International*, 190(3), 1455-1463.

Hasan, M., Shang, Y., & Jin, W. (2018). Delineation of weathered/fracture zones for aquifer potential using an integrated geophysical approach: A case study from South China. *Journal of Applied Geophysics*, 157, 47-60.

Hussain Y., et al 2020B. Characterization of Sobradinho landslide in fluvial valley using MASW and ERT methods, *REM - International Engineering Journal* (in press).

Hussain, Y., Moura, C., Borges, W., 2020A. Estimation of total groundwater reserves and delineation of weathered/fault zones for aquifer potential: a case study from Federal District, BRAZIL, *Earth and Space Science Open Archive*, DOI: 10.1002/essoar.10503440.

Jamal, N., & Singh, N. P. (2018). Identification of fracture zones for groundwater exploration using very low frequency electromagnetic (VLF-EM) and electrical resistivity (ER) methods in hard rock area of Sangod Block, Kota District, Rajasthan, India. *Groundwater for Sustainable Development*, 7, 195-203.

Jin-long, L., Hamza, O., Davies-Vollum, K. S., & Jie-qun, L. (2018). Repairing a shield tunnel damaged by secondary grouting. *Tunnelling and Underground Space Technology*, 80, 313-321.

Kavouri, K., Plagnes, V., Tremoulet, J., Dörfliger, N., Rejiba, F., & Marchet, P. (2011). PaPRIKa: a method for estimating karst resource and source vulnerability—application to the Ouyse karst system (southwest France). *Hydrogeology Journal*, 19(2), 339-353.

Krawczyk, C. M., Polom, U., Trabs, S., & Dahm, T. (2012). Sinkholes in the city of Hamburg—New urban shear-wave reflection seismic system enables high-resolution imaging of subsurface structures. *Journal of Applied Geophysics*, 78, 133-143.

Kruse, S., Grasmueck, M., Weiss, M., & Viggiano, D. (2006). Sinkhole structure imaging in covered karst terrain. *Geophysical Research Letters*, 33(16).

Lapenna, V., Lorenzo, P., Perrone, A., Piscitelli, S., Rizzo, E., & Sdao, F. (2005). 2D electrical resistivity imaging of some complex landslides in Lucanian Apennine chain, southern Italy. *Geophysics*, 70(3), B11-B18.

CALVO EM (2015) Preliminary environmental characterization and conservation proposal to gruta da tarimba karst system – Goiás state, Brazil.

Loke MH (2004) Tutorial: 2-D and 3-D electrical imaging surveys. Geotomo Software.

Gambetta, M., Armadillo, E. G. I. D. I. O., Carmisciano, C. O. S. M. O., Stefanelli, P. A. O. L. O., Cocchi, L. U. C. A., & Tontini, F. C. (2011). Determining geophysical properties of a near-surface cave through integrated microgravity vertical gradient and electrical resistivity tomography measurements. *Journal of cave and karst studies*, 73(1), 11-15.

Martinez-Lopez, J., Rey, J., Duenas, J., Hidalgo, C., & Benavente, J. (2013). ELECTRICAL TOMOGRAPHY APPLIED TO THE DETECTION OF SUBSURFACE CAVITIES. *Journal of Cave & Karst Studies*, 75(1).

Martínez-Moreno, F. J., Pedrera, A., Ruano, P., Galindo-Zaldívar, J., Martos-Rosillo, S., González-Castillo, L., ... & Marín-Lechado, C. (2013). Combined microgravity, electrical resistivity tomography and induced polarization to detect deeply buried caves: Algaídilla cave (Southern Spain). *Engineering Geology*, 162, 67-78.

Mohamed, A. M. E., El Hussain, I., Deif, A., Araffa, S. A. S., Mansour, K., & Al Rawas, G. (2019). Integrated ground penetrating radar, electrical resistivity tomography and multichannel

analysis of surface waves for detecting near surface caverns at Duqm area, Sultanate of Oman. *Near Surface Geophysics*, 17(4), 379-401.

Ndatuwong, L. G., & Yadav, G. S. (2014). Identifications of fractured zones in part of hard rock area of Sonebhadra District, UP, India using integrated surface geophysical method for groundwater exploration. *Arabian Journal of Geosciences*, 7(5), 1781-1789.

Ozegin, K. O., Oseghale, A. O., & Ogedegbe, E. O. (2012). Integrated geophysical investigation and characterisation of aquifer structures in a complex environment. *Advances in Applied Science Research*, 3(1), 475-480.

Pazzi, V., Di Filippo, M., Di Nezza, M., Carlà, T., Bardi, F., Marini, F., ... & Fanti, R. (2018). Integrated geophysical survey in a sinkhole-prone area: Microgravity, electrical resistivity tomographies, and seismic noise measurements to delimit its extension. *Engineering Geology*, 243, 282-293.

Pirttijarvi, M. (2004) Manual of the KHFFILT program; Karous-Hjelt and Fraser filtering of VLF measurements, Version 1.1a. University of Oulu, Finland.

Anchuela, Ó. P., Julián, P. L., Sainz, A. C., Liesa, C. L., Juan, A. P., Cordero, J. R., & Benedicto, J. P. (2015). Three dimensional characterization of complex mantled karst structures. Decision making and engineering solutions applied to a road overlying evaporite rocks in the Ebro Basin (Spain). *Engineering Geology*, 193, 158-172.

PUTIŠKA, R., KUŠNIRÁK, D., Dostal, I., LAČNÝ, A., MOJZESS, A., Hok, J., ... & BOŠANSKÝ, M. (2014). INTEGRATED GEOPHYSICAL AND GEOLOGICAL INVESTIGATIONS OF KARST STRUCTURES IN KOMBEREK, SLOVAKIA. *Journal of Cave & Karst Studies*, 76(3).

Putiška, R., Sabol, M., Kušnirák, D., & Dostál, I. (2017). Geophysical Research at the Prepoštská Cave and Čertova Pec Cave Neanderthal Sites (Western Slovakia). *Archaeological Prospection*, 24(2), 119-131.

Sasaki, Y. (1992). RESOLUTION OF RESISTIVITY TOMOGRAPHY INFERRED FROM NUMERICAL SIMULATION 1. *Geophysical prospecting*, 40(4), 453-463.

Sharma S.P., and Singh A. (2016) Advancement in 2D interpretation approach in very low frequency electromagnetic measurement, 23rd Electromagnetic Induction in the Earth Workshop, Chiang Mai, Thaila.

Sharma, S. P., & Baranwal, V. C. (2005). Delineation of groundwater-bearing fracture zones in a hard rock area integrating very low frequency electromagnetic and resistivity data. *Journal of Applied geophysics*, 57(2), 155-166.

Silva, O. L., Bezerra, F. H., Maia, R. P., & Cazarin, C. L. (2017). Karst landforms revealed at various scales using LiDAR and UAV in semi-arid Brazil: Consideration on karstification processes and methodological constraints. *Geomorphology*, 295, 611-630.

Smith, D. L. (1986). Application of the pole-dipole resistivity technique to the detection of solution cavities beneath highways. *Geophysics*, 51(3), 833-837.

Strelec, S., Mesec, J., Grabar, K., & Jug, J. (2017). Implementation of in-situ and geophysical investigation methods (ERT & MASW) with the purpose to determine 2D profile of landslide. *Acta Montanistica Slovaca*, 22(4), 345-358.

Husein, A., Prasetyo, H., Bahri, A. S., Santos, F. A. M., & Santosa, B. J. (2014). The VLF-EM imaging of potential collapse on the LUSI embankment. *Journal of Applied Geophysics*, 109, 218-232.

Neto, P. X., & de Medeiros, W. E. (2006). A practical approach to correct attenuation effects in GPR data. *Journal of Applied Geophysics*, 59(2), 140-151.

Youssef, A. M., Al-Harbi, H. M., Gutiérrez, F., Zabramwi, Y. A., Bulkhi, A. B., Zahrani, S. A., ... & El-Haddad, B. A. (2016). Natural and human-induced sinkhole hazards in Saudi Arabia: distribution, investigation, causes and impacts. *Hydrogeology Journal*, 24(3), 625-644.

Zhou, W., Beck, B. F., & Adams, A. L. (2002). Effective electrode array in mapping karst hazards in electrical resistivity tomography. *Environmental geology*, 42(8), 922-928.